ANALYSIS OF A SCALABLE PRECONDITIONER FOR THE WIGNER-POISSON EQUATION *

M. S. LASATER†, C. T. KELLEY‡, A. G. SALINGER§, D. L. WOOLARD¶, G. RECINE‖, AND P. ZHAO**

Abstract. We analyze a preconditioner for the time-independent Wigner-Poisson equations for a resonant tunneling diode and present a numerical example of a continuation study which supports the theory. The application of the preconditioner transforms the equations into a compact fixed point problem for the Wigner distribution. After discretization, the Jacobians of the discrete problem have mesh-independent eigenvalue clustering properties, which implies the mathematical scalability of the nonlinear solver.

Key words. Wigner-Poisson Equations, Scalable Preconditioner, Integral Equation, Continuation, Resonant Tunneling Diode

AMS subject classifications. 65H10, 65H20, 45G10, 65F10, 81S30

1. Introduction. In this paper we analyze a scalable preconditioner for the Wigner-Poisson equations for a resonant tunneling diode (RTD). We have applied this preconditioner in previous continuation studies [17–21, 28], and our intent in this paper is to analyze the scalability of the preconditioner. The principal contribution of this paper is the identification of the appropriate Banach space setting to enable us to prove collective compactness [1] of the sequence of discretized preconditioned problems, which will imply scalability of the overall Newton-GMRES solver and the continuation.

The Wigner-Poisson equations [4, 25] are a system comprised of an integro-partial differential equation (1.1) for the distribution of the electrons in the device and Poisson's equation (1.8) for the electrostatic potential.

We begin this section with a brief account of the physics of an RTD in § 1.1 and present the Wigner-Poisson equations in § 1.2. In § 2 we present some results from [16, 18] which illustrate the scalability in a parallel continuation application. In § 3 we show how to transform the Wigner-Poisson equations into a compact fixed point problem on a certain Banach space, and conclude that the Fréchet derivative of the transformed problem has a countable sequence of eigenvalues clustering at zero. In § 4 we use classical results from Anselone [1] to connect the infinite dimensional analysis in § 3 to the discretization and the continuation method used in [17–21, 28].

1.1. Resonant Tunneling Diodes. An RTD is created by joining different semiconductor materials into a heterostructure. The flow of electrons under an imposed voltage bias is a function of the material properties of the semiconductor. A semiconductor contains two types of electrons: valence electrons and free electrons. The valence electrons are those involved in the covalent bonds between the atoms in the semiconductor, and free electrons are those that can freely move about the semiconductor. The state of an electron is determined by its energy; those with enough energy are free electrons while those with low energy are valence electrons. The energy difference between the highest energy valence electrons and the lowest energy free electrons is known as the band gap. In the construction of an RTD, the different semiconductor materials have different band gaps, and the sections of the RTD which are made with a semiconductor that

*Version of April 4, 2007. This research was supported in part by U. S. Army Research Office grants DAAD19-01-1-0592, W911NF-04-1-0276, W911NF-06-1-0096, and W911NF-05-1-0171, and National Science Foundation grants DMS-0070641, DMS-0209695, and DMS-0404537.

† MIT Lincoln Laboratory, 244 Wood St, Lexington, MA 02420-9108, USA (mlasater@ll.mit.edu)

‡ North Carolina State University, Center for Research in Scientific Computation and Department of Mathematics, Box 8205, Raleigh, N. C. 27695-8205, USA (Tim_Kelley@ncsu.edu)

§ Sandia National Laboratories P.O. Box 5800, MS-1111 Albuquerque, New Mexico, 87185, USA Sandia is a multiprogram laboratory operated by Sandia Corporation, a Lockheed-Martin Company, for the United States Department of Energy under Contract DE-AC04-94AL85000 (agsalin@sandia.gov)

¶ U. S. Army Research Office U. S. Army Research Laboratory, RTP, North Carolina, 27709-2211, USA (woolard@us.army.mil)

‖Stevens Institute of Technology, Department of Physics, Hoboken, NJ 07030 (greg@phy.stevens.edu)

** Electrical and Computer Engineering Department North Carolina State University, Raleigh, North Carolina, 27695-8205, USA (pzhao@eos.ncsu.edu)

has a higher band gap than the surrounding semiconductor material will require more energy to transverse than the surrounding areas. This additional energy effectively creates potential barriers within the RTD. Figure 1.1 shows the structure of the RTD we are modeling as well as the electric potential, denoted by $U(x)$, within the RTD.

FIG. 1.1. *Resonant Tunneling Diode and Its Electric Potential U*

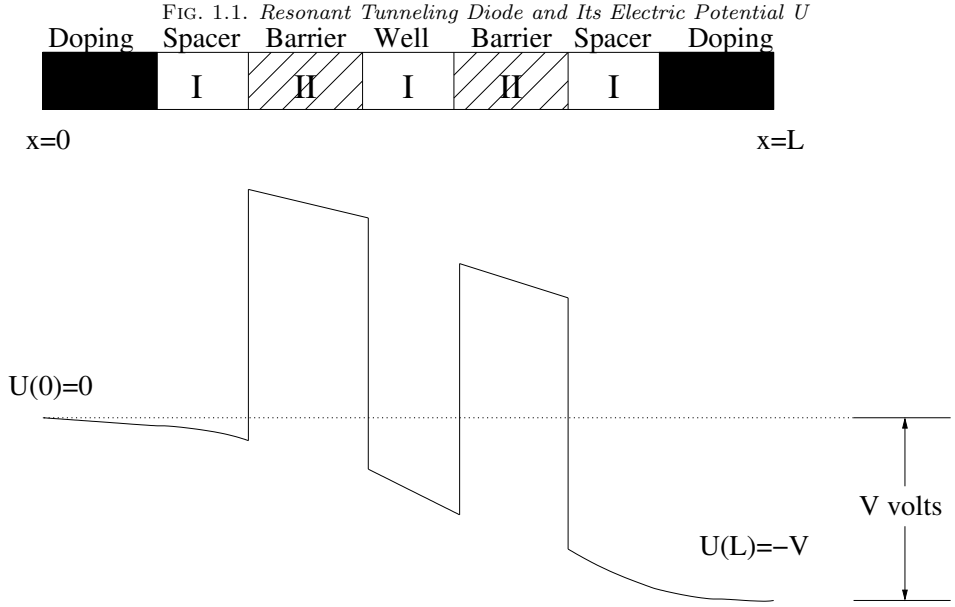

Here, semiconductor material I (for our simulations, we use gallium arsenide) is chosen to have a lower band gap than semiconductor material II (for our simulations, we use gallium aluminum arsenide). Note that there is a region of semiconductor material I between areas of semiconductor material II. This region is known as a quantum well since it is surrounded by potential barriers on both sides.

As shown in Figure 1.1, the left side of the RTD is grounded (that is, $U(0) = 0$) while there is a voltage drop of V volts at the right side (that is, $U(L) = -V$). Since electrons want to be at a lower potential energy, they begin traveling from the left side of the RTD to the right side. In classical physics, electrons are treated as particles. Classically, if the electrons do not have enough energy as they approach the potential barriers, they will reflect off the barriers and move back to the left. In quantum mechanics, electrons are treated as waves. This means no matter how much energy an electron has as it is approaching the potential barriers, there is a probability of the electron passing through the barriers and reaching the other side. This phenomenon is known as quantum tunneling and is the basis for the device's operation.

1.2. The Equations. This paper is concerned with the time-independent form of the equations. We write the integro-partial differential equation as

$$W(f) = Df + P(f) + S(f) = 0. \tag{1.1}$$

In (1.1) $f = f(x, k)$, is the distribution of the electrons, $x \in [0, L]$ is the spatial coordinate, $k \in (-K, K)$ is momentum, and L is the length of the device. The bounds on momentum in § 2.2 in this paper are $K = .25$ inverse angstroms [16]. Similar bounds have been used in [3, 7].

The linear term Df on the right side of (1.1) represents the kinetic energy effects on the distribution and is given by

$$Df = -\frac{hk}{2\pi m^*}\frac{\partial f}{\partial x}. \tag{1.2}$$

In (1.2), h is Planck's constant, and m^* is the effective mass of the electron. The second term, $P(f)$, is the

nonlinear term in the equation and accounts for the potential energy effects on the distribution

$$P(f) = -\frac{4}{h}\int_{-K}^{K} f(x,k')T(x,k-k')dk'. \tag{1.3}$$

The function $T(x,k)$ is defined by

$$T(x,k) = \int_0^{\frac{L_c}{2}} [U(x+y) - U(x-y)]\sin(2yk)dy. \tag{1.4}$$

In this equation, $U(x)$ is the electric potential as a function of position, and L_c is the correlation length. This term is nonlinear in f because $U(x)$ depends on f through Poisson's equation (see (1.8) and (1.10)). The last term describes electron-electron scattering

$$S(f) = \frac{1}{\tau}\left[\frac{\int_{-K}^{K} f(x,k')dk'}{\int_{-K}^{K} f_0(x,k')dk'} f_0(x,k) - f(x,k)\right] \tag{1.5}$$

In (1.5), τ is the relaxation time, and $f_0(x,k)$ is the equilibrium Wigner distribution. f_0 is the solution of (1.1) when there is no voltage difference (zero-bias) across the device. The equations for f_0 differ both in form and in analytic properties from those for the nonzero-bias case.

Boundary conditions are imposed at the device edges to describe the distribution of electrons entering the device. On the left ($x = 0$), we have for $k > 0$ (electrons with positive momentum that are moving right)

$$f(0,k) = f_\ell(k) = \frac{4\pi m^* k_B T}{h^2}\ln\left(1 + \exp\left[\frac{1}{k_B T}\left(\frac{h^2k^2}{8\pi^2 m^*} - \mu\right)\right]\right). \tag{1.6}$$

Similarly on the right ($x = L$), we specify f for $k < 0$ (electrons with negative momentum that are moving left)

$$f(L,k) = f_r(k) = \frac{4\pi m^* k_B T}{h^2}\ln\left(1 + \exp\left[\frac{1}{k_B T}\left(\frac{h^2k^2}{8\pi^2 m^*} - \mu\right)\right]\right). \tag{1.7}$$

In (1.6) and (1.7), k_B is Boltzmann's constant, T is the temperature, μ is the Fermi energy at the endpoints.

The electric potential $U(x)$ is the sum of the potential barrier $\Delta_c(x)$ that arises from the heterojunction of the two different semiconductor materials and the electrostatic potential $u(x)$. The electrostatic potential is the solution of Poisson's equation

$$\frac{d^2u}{dx^2} = \frac{q^2}{\epsilon}\left[N_d(x) - \frac{1}{2\pi}\int_{-K}^{K} f(x,k')dk'\right]. \tag{1.8}$$

In (1.8), q is the charge of the electron, ϵ is the dielectric constant, and $N_d(x)$ is the doping profile. N_d is piecewise constant with a small number (≤ 10) of discontinuities. The boundary conditions for (1.8) are

$$u(0) = 0, u(L) = -V_{bias}, \tag{1.9}$$

where $V_{bias} \geq 0$ is the applied voltage (bias). The potential U is given by

$$U(x) = u(x) + \Delta_c(x), \tag{1.10}$$

where $\Delta_c(x)$ is piecewise constant with a small number of discontinuities.

We will assume that the structure is symmetric about $x = \frac{L}{2}$, *i. e.*

$$N_d(x) = N_d(L-x) \text{ and } \Delta_c(x) = \Delta_c(L-x). \tag{1.11}$$

To evaluate the integral in (1.4) we must extend U outside of the interval $[0, L]$. We do this by defining $U(x) = U(L)$ for $x > L$ and $U(x) = U(0)$ for $x < 0$. With this definition, U is a piecewise smooth function of x, having discontinuities where Δ_c does.

In the zero-bias case we seek to find f_0. The equations differ from those for the nonzero-bias ($V > 0$) case in that the collision term is missing from the integro-partial differential equation, resulting in

$$W(f) = Df + P(f) = 0, \tag{1.12}$$

and $V = 0$ in the boundary conditions (1.9) for the Poisson equation. We will see in § 3 that the compactness properties of the preconditioned operator are more favorable in this case.

In the next section, we will discuss a previous continuation study performed with the Wigner-Poisson equations that demonstrates the scalability of our preconditioner. To solve the Wigner-Poisson equations numerically, we approximated integrals in x with a Riemann sum, integrals in k with the composite midpoint rule, solved (1.8) with a central difference, and discretized the spatial differential operator with the second-order BDF scheme [2]. The mesh spacing in x and k is uniform, with the x-space of $[0, L]$ divided into $N_x - 1$ intervals of length $\Delta_x = L/(N_x - 1)$ and the k-space of $(-K, K)$ divided into an even number N_k intervals of length $\Delta_k = 2 * K/N_k$.

2. Continuation Study.

2.1. Continuation. The objective of our earlier work [17–21, 28] was to do a continuation study with V_{bias} as the parameter. There are fold singularities in the range of interest, and the standard approach for resolving such singularities is pseudo-arclength continuation [11]. The approach begins with solving for f_0. Then one introduces an artificial "arc length" parameter s, treats the natural parameter V_{bias} as an unknown, and solves the extended system

$$\mathcal{F}(f, V_{bias}) = \begin{pmatrix} \mathcal{M}W(f) \\ \mathcal{N}(f, V_{bias}, s) \end{pmatrix} = \begin{pmatrix} 0 \\ 0 \end{pmatrix}. \tag{2.1}$$

In (2.1), $\mathcal{M}W(f)$ is the equation (1.1) (which specifies f to be a steady-state Wigner distribution) multiplied by a precondtioning matrix $\mathcal{M}$. The specific preconditioning matrix used is discussed in § 3. In (2.1), we want to solve $\mathcal{N}(f, V_{bias}, s)$ is a scalar normalization condition. One example of such a condition is

$$\mathcal{N}(f, V_{bias}, s) = (\dot{f}, f - f_{prev}) + \dot{V}_{bias}(V_{bias} - V_{bias,prev}) - ds \tag{2.2}$$

where $\dot{f}$ and $\dot{V}_{bias}$ are approximations to the derivatives of f and V_{bias} with respect to s, and the subscript *prev* refers to the previous point on the path.

2.2. Numerical Results. Here we present some results from [16] to illustrate the scalabilty. We used Sandia National Laboratories' Trilinos [9] framework, and in particular the LOCA [23] continuation code, for the computation, where a Newton-GMRES [13, 14] method was used to solve the nonlinear equations arising during the continuation. This is a variant of Newton's method in which the equation for the Newton direction is solved with GMRES [22], and the inner GMRES iteration is terminated when the relative linear residual is sufficiently small. In Table 2.2 we tabulate the Newton iterations per step in arc length and the GMRES iterations per Newton as functions of N_x and N_k. The number of GMRES iterations per Newton step are roughly constant, which indicates that the preconditioner is mathematically scalable. The remainder of the paper fills in the theory behind why our preconditioner is scalable.

Table 2.1 list the values of the physical constants for this simulation.

TABLE 2.1
Physical Constants

Symbol	Name	Numerical Value	Units
h	Planck's Constant	4.135667	$(eV * fs)$
m^*	Effective Mass of Electron	0.003778	$\frac{eV * fs^2}{\mathring{A}^2}$
k_B	Boltzmann's Constant	8.617343×10^{-5}	$\frac{eV}{K}$
T	Temperature	77	K
μ	Fermi Energy at Endpoints	0.0863814496	eV
K	Bound on Momentum	0.25	$\mathring{A}^{-1}$
L	Length of Device	550	$\mathring{A}$
τ	Relaxation Time	525	fs
ϵ	Dielectric Permittivity	7.144×10^{-2}	$\frac{C^2}{eV * fs}$
q	Charge of Electron	1.6×10^{-19}	C

TABLE 2.2
GMRES iterations per Newton iteration

N_x	N_k	Avg. New./ds	Avg. Kry./New.
86	72	2.6	176
172	144	2.5	174
344	288	2.5	173
688	576	2.5	186

3. Compactness. In this section we begin by formulating the preconditioned operators. We then show that these operators are completely continuous on the appropriate Banach spaces. By this we mean [1, 10] that the image of the unit ball is mapped to a precompact set by the operator.

The spaces and the analysis differ for the zero and nonzero-bias problems, so we treat them separately in § 3.2 and § 3.3. However, the two cases share the map P, which we consider in § 3.1.

We begin by rewriting the equation in the zero-bias case as

$$-Df = P(f). \tag{3.1}$$

We can then use the boundary conditions (1.6) and (1.7) to invert the differential operator on the left side of the equation to obtain the fixed point problem. Applying D^{-1} to both sides of (3.1) transforms (3.1) into the fixed point problem

$$f = Z_0(f) = -D^{-1}P(f) = A(f) + b, \tag{3.2}$$

where $A(f)(x,k)$ is defined as

$$A(f)(x,k) = \begin{cases} \frac{-B}{k}\int_0^x \int_{-K}^K f(z,k')T(z,k-k')dk'dz & k > 0 \\ \\ \frac{B}{k}\int_x^L \int_{-K}^K f(z,k')T(z,k-k')dk'dz & k < 0 \end{cases} \tag{3.3}$$

$$B = \frac{8\pi m^*}{h^2}, \tag{3.4}$$

and

$$b(x,k) = \begin{cases} f_\ell(k) & k > 0 \\ f_r(k) & k < 0 \end{cases}.$$

In § 3.2 we will show that Z_0 is a completely continuous map on

$$X_0 = \{f \in C([0,L]\times[-K,K]) | f(x,k) = f(x,-k), f(x,k) = f(L-x,k)\}, \tag{3.5}$$

which is a closed subspace of $C([0,L]\times[-K,K])$.

In the nonzero-bias case we write the equation as

$$(I - \tau D)f = \tau P(f) + Q(f), \tag{3.6}$$

where Q is defined by

$$Q(f)(x,k) = \frac{\int_{-K}^K f(x,k')dk'}{\int_{-K}^K f_0(x,k')dk'} f_0(x,k). \tag{3.7}$$

We then use (1.6) and (1.7) to invert the differential operator, as we did in the zero-bias case. We obtain the fixed point problem

$$f = Z(f) = (I - \tau D)^{-1}(\tau P(f) + Q(f)). \tag{3.8}$$

We will show in § 3.3 that Z is completely continuous on the space X of functions which are L^2 in k and continuous in x. The norm on X is

$$\|f\|_X = \sup_{0\le x\le L}\left(\int_{-K}^{K} f(x,k')^2 dk'\right)^{1/2}. \tag{3.9}$$

For both cases, complete continuity of the operator will imply that the Fréchet derivative is a compact linear operator on the Banach space. This is the tool we will need to show in § 4 that a preconditioned Newton-GMRES solver will be mathematically scalable, in the sense that the number of Krylov iterations needed to reduce the residual by a given amount is independent of the discretization.

3.1. Properties of the map P. The design of the preconditioner will exploit properties of the maps from f to U and from f to T, which we summarize in Lemma 3.1. In the statement of the lemma, and throughout the paper, we will denote $L^2([0,L]\times[-K,K])$ simply by L^2 and the space $C([0,L]\times[-K,K])$ simply by C.

LEMMA 3.1. *The map from f to U is an affine compact map from both L^2 or X to the subspace PC_d of $L^\infty([0,L])$ of piecewise continuous functions with discontinuities only at those of Δ_c. The map from f to T is a compact affine map from L^2, X, or X_0 to C.*

Proof. The well-known properties of the Green's function for the second derivative operator [24] imply that the map from f to u is a compact map from L^2, X, or X_0 to $C([0,L])$. The assertions in the lemma follow from that compactness. □

Lemma 3.1 implies that P maps X continuously into C, but not compactly, because the variable x is not integrated in (1.3). However the image of the unit ball in either L^2, X, or X_0 is a bounded set in $C([0,L]\times[-K,K])$ which is equicontinuous in k, and hence compact by the Ascoli theorem.

3.2. The Zero-Bias Case. In this section we prove

THEOREM 3.2. *Let $V=0$ and let Z_0 be defined by* (3.2) *and* (3.3). *Then Z_0 is a completely continuous map on X_0.*

Proof. The symmetry assumptions (1.11) and the zero-boundary conditions ($V=0$ in (1.9)) imply that if $f\in X_0$, then $U(x)=U(L-x)$. Hence,

$$T(x,k) = -T(x,-k) \text{ and } T(L-x,k) = T(x,k), \tag{3.10}$$

for all k and x.

If $f\in X_0$, then f is even in k and so

$$\int_{-K}^{K} f(x,k')T(x,k')=0$$

and hence $P(f)(x,0)=0$. Since $P(f)$ is analytic in k, the integrals on the right side of (3.3) are continuous functions of k, even at $k=0$. Combining this with (3.10) implies that A maps X_0 into itself. Since $b\in X_0$, we have shown that Z_0 maps X_0 continuously into itself.

To demonstrate the compactness, we must demonstrate equicontinuity in both variables. We do this for $k\ge 0$; the proof for $k\le 0$ is the same. We use the evenness of f in k to write

$$A(f)(x,k) = \frac{-B}{k}\int_0^x\int_0^K f(z,k')(T(z,k-k')+T(z,k+k'))dk'dz.$$

The definition of T implies that

$$\frac{T(z,k-k')+T(z,k+k')}{k}$$

is a uniformly continuous function in (z,k,k'). Hence A maps bounded sets in X_0 into sets of functions which are equicontinuous in k. The equicontinuity in x and both variables together follows from the integration in z. □

3.3. The Nonzero-Bias Case. The symmetry that we used to show compactness of A is not present in the nonzero-bias case. Moreover, the solution need not be continuous in k if $x = 0$. Hence we must use the larger space X (defined in (3.9)).

The compactness result is

THEOREM 3.3. *Let $Z(f)$ be given by* (3.8)*. Then $Z(f)$ is a completely continuous map on X.*

Proof. Recall that

$$Q(f)(x,k) = \frac{\int_{-K}^{K} f(x,k')dk'}{\int_{-K}^{K} f_0(x,k')dk'} f_0(x,k).$$

Q is a bounded operator from X into C if $f_0 \in C$, which we will assume. Q is not compact, because the x variable is not integrated.

Therefore the image of $\tau P + Q$ of the unit ball in X is a family of functions in C which is bounded, equicontinuous in k, but not equicontinuous in x. Hence that image is not a compact set in C.

As we did in the zero-bias case, we show that the application of $(I - \tau D)^{-1}$ will make the map compact. We can obtain a closed form expression for $(I - \tau D)^{-1}$ by using the boundary data (1.6)–(1.7). For $g \in C$,

$$(I-\tau D)^{-1} g(x,k) = \begin{cases} \frac{-\bar{c}}{k} \int_0^x e^{\bar{c}(z-x)/k} g(z,k)\, dz + e^{-\bar{c}x/k} f_l(k) & k > 0 \\ \\ \frac{\bar{c}}{k} \int_x^L e^{\bar{c}(x-z)/k} g(z,k)\, dz + e^{\bar{c}(L-x)/k} f_r(k) & k < 0 \end{cases} . \tag{3.11}$$

Here

$$\bar{c} = \frac{2\pi m^*}{\tau h}.$$

In view of the properties of the map $\tau P + Q$, we can complete our proof of compactness if we show that the integral operator V defined on $C([0,L])$ by

$$V(w)(x,k) = \begin{cases} \frac{\bar{c}}{k} \int_0^x e^{\bar{c}(z-x)/k} w(z)\, dz & k > 0 \\ \\ \frac{-\bar{c}}{k} \int_x^L e^{\bar{c}(x-z)/k} w(z)\, dz & k < 0 \end{cases} \tag{3.12}$$

is a compact operator from $C[0,L]$ into X. We prove this by showing that V is the limit in the operator norm of the operators $\{V_\delta\}$, where

$$V_\delta(w)(x,k) = \begin{cases} \frac{\bar{c}}{k+\delta} \int_0^x e^{\bar{c}(z-x)/k} w(z)\, dz & k > 0 \\ \\ \frac{-\bar{c}}{k-\delta} \int_x^L e^{\bar{c}(x-z)/k} w(z)\, dz & k < 0 \end{cases} . \tag{3.13}$$

The operators V_δ are Volterra integral operators with continuous kernels, and are therefore compact.

Let $w \in C[0,L]$. We have for $k > 0$

$$\begin{aligned} |(V - V_\delta)(w)(x,k)| &\leq \bar{c} \tfrac{\delta}{k(\delta+k)} \int_0^x |w(z)| e^{\bar{c}(z-x)/k}\, dz \\ &\leq \bar{c} \|w\|_\infty \tfrac{\delta}{\delta+k} (1 - e^{-\bar{c}x/k}) \end{aligned}$$

A similar analysis holds for $k < 0$, hence

$$\|(V - V_\delta)(w)\|_X \leq \|w\|_\infty \sqrt{2\delta}, \tag{3.14}$$

which completes the proof.

□

We conclude this section with some remarks on the smoothness properties of Z and Z_0, and the solutions f and f_0. The maps Z and Z_0 are quadratic in f, this means that the Fréchet derivatives Z' and Z_0' of Z and Z_0 are uniformly Lipschitz continuous, *i. e.* there is γ such that for all $f, g \in X$

$$\|Z'(f) - Z'(g)\| \leq \gamma \|f - g\|,$$

with a similar statement holding for Z_0'.

We have also shown that Z maps X into

$$Y^1 = C^1([0,L]\times[-K,0)\cup(0,K])\cap L^\infty([0,L]\times[-K,K]).$$

and hence any solution of $f = Z(f)$ must be in Y^1.

4. Discretization and Scalability. The results in this section are a straightforward application of classical theorems on collective compactness [1] and results that relate spectral clustering to the performance of GMRES [5].

As previously stated, we will solve the discretized forms of equations (3.2) and (3.8) with a Newton-GMRES method. We express the ideas in some generality so that we can include both the zero and nonzero-bias cases. For example, if we seek to solve a compact fixed point problem of the form

$$u - W(u) = 0 \tag{4.1}$$

where W is completely continuous, then the Newton step is the solution of the linear equation

$$s - W'(u)s = -(u - W(u)). \tag{4.2}$$

We solve (4.2) with GMRES, terminating the linear iteration when the inexact Newton condition [6, 13, 14]

$$\|s - W'(u)s + (u - W(u))\| \le \eta\|u - W(u)\| \tag{4.3}$$

holds. In (4.3), the norm $\|\cdot\|$ is the norm associated with the scalar product used to define orthogonality within the GMRES algorithm. The number of iterations needed to satisfy (4.3) can be related to the spectral clustering of W' [5].

There is a subtle issue here. Assume one uses the L^2 inner product to implement GMRES. The maps Z and Z_0 are not defined on L^2, but on the spaces X and X_0. Moreover, the derivatives are also not defined on L^2. Hence a discussion of the performance of GMRES is only meaningful in the context of finite dimensional approximations, which is the setting of the analysis in what follows.

If we approximate matrix-vector products with forward differences, then each linear iteration will cost one new evaluation of the nonlinear map. This means that the theoretical (or mathematical) scalablilty of the method will follow from a bound on the number of GMRES iterations needed for each nonlinear iteration.

We will obtain such a bound by extending the discrete maps to the appropriate function spaces via interpolation and restriction operators, which we define in § 4.2. We must show that the spectral properties of the Fréchet derivatives of the extended maps are the same as those of the discrete maps, which they will be if interpolations and restrictions are based on the same nodal values as the discretization. If the discretization is convergent, then the extended maps will converge strongly to the infinite dimensional map. We can then complete the analysis by showing that the extended maps are collectively compact, because we can then apply the theory in [1] to argue that the spectral properties of the Jacobians of the discrete problems are inherited by those of the infinite dimensional problems, for which we have proved compactness in § 3. Then we can use the resolvent integration results from [5, 15, 26] to derive a bound for the number of linear iterations in terms of the eigenvalues of the Fréchet derivative of the infinite dimensional problem and the termination criterion applied to the linear solver.

We do this in stages. We begin in § 4.1 by reviewing the relevant results from [1, 5] and defining the essential ideas. We then state a theorem that is a blend of results from [1, 5]. Then in § 4.2 we show how the discrete approximations to Z and Z_0 can be expressed as maps on the function spaces X and X_0. In § 4.3 we will show that the the approximate maps on the function spaces are collectively compact families of operators.

4.1. Spectral Clustering. Following [1] we say that a set of maps $\{W^{\mathbf{\Delta}}\}$ on a Banach space $\mathcal{B}$ is *collectively compact* if for any bounded set $D \subset \mathcal{B}$ there is a compact set $\mathcal{K} \subset \mathcal{B}$, such that $W^{\mathbf{\Delta}}(D) \subset \mathcal{K}$ for all $\mathbf{\Delta}$. Here $\mathbf{\Delta}$ is a vector of discretization parameters, partially ordered in the component-wise sense, with $\mathbf{\Delta} < \tilde{\mathbf{\Delta}}$ meaning that $\mathbf{\Delta}$ is a finer or more accurate discretization than $\tilde{\mathbf{\Delta}}$. The family is *strongly*

convergent if $W^{\mathbf{\Delta}}(u) \to W(u)$ as $\mathbf{\Delta} \to 0$ for all $u \in \mathcal{B}$. The family is *equidifferentiable* if each $W^{\mathbf{\Delta}}$ is Fréchet differentiable and the remainder in the Taylor expansion

$$W^{\mathbf{\Delta}}(u+y) - W^{\mathbf{\Delta}}(u) - W^{\mathbf{\Delta}'}(u)y$$

is $o(\|y\|)$ independently of $\mathbf{\Delta}$. Examples of families of strongly convergent, collectively compact, and equidifferentiable maps include standard discretizations of nonlinear integral operators, and we will show in the following sections that natural discretizations of Z and Z_0 are can be expressed as such families.

We note that equidifferentiability follows from uniform Lipschitz continuity of $W^{\mathbf{\Delta}'}$ on bounded sets in $\mathcal{B}$, and we will use that condition rather than equidifferentiability in the statements that follow.

We summarize the results from [1] we need in Theorem 4.1.

THEOREM 4.1. *Let $\{W^{\mathbf{\Delta}}\}$ be a family of strongly convergent (to W), collectively compact maps on a Banach space $\mathcal{B}$. Assume that the maps $W^{\mathbf{\Delta}'}$ are uniformly Lipschitz continuous on bounded sets in $\mathcal{B}$. Then for all $u \in \mathcal{B}$ the Fréchet derivatives $W^{\mathbf{\Delta}'}(u)$ are strongly convergent (to $W'(u)$) collectively compact families of linear operators, and for all $u \in \mathcal{B}$ and $\epsilon > 0$ there is $\mathbf{\Delta}_0$ such that the spectrum of $W^{\mathbf{\Delta}'}(u)$ is within ϵ of the spectrum of $W'(u)$ for all $\mathbf{\Delta} \leq \mathbf{\Delta}_0$.*

Our scalability results use Theorem 4.1 to argue that the spectral properties of W' govern the convergence of the GMRES iteration for the Newton step for the approximate problem

$$u - W^{\mathbf{\Delta}}(u) = 0. \tag{4.4}$$

To do this we must specify the scalar product used in the GMRES iteration and make some assumptions on the maps $W^{\mathbf{\Delta}}$ that go beyond the assumptions needed in Theorem 4.1. We assume that there are finite dimensional subspaces $\mathcal{B}_{\mathbf{\Delta}}$ of $\mathcal{B}$ and projections $\mathcal{P}^{\mathbf{\Delta}} : \mathcal{B} \to \mathcal{B}_{\mathbf{\Delta}}$ such that

$$W^{\mathbf{\Delta}}(u) = \mathcal{P}^{\mathbf{\Delta}} W^{\mathbf{\Delta}}(\mathcal{P}^{\mathbf{\Delta}} u). \tag{4.5}$$

The identity (4.5) says that $W^{\mathbf{\Delta}}$, while defined on all of $\mathcal{B}$, only really acts on the subspace $\mathcal{B}_{\mathbf{\Delta}}$, hence a solution of (4.4) must lie in $\mathcal{B}_{\mathbf{\Delta}}$. We will implement GMRES using any scalar product on $\mathcal{B}_{\mathbf{\Delta}}$, and let $\|\cdot\|_{\mathbf{\Delta}}$ be the corresponding norm. Note that $\mathcal{B}$ need not be a Hilbert space, and our scalar product is only used to specify the notion of orthogonality within the GMRES algorithm.

Now let $N(\rho, \mathbf{\Delta}, u)$ denote the number (counted by algebraic multiplicity) of eigenvalues of $I - W^{\mathbf{\Delta}'}(u)$ which are outside the disk of radius ρ about 1. Theorem 4.1 implies that for any fixed $\rho > 0$, $N(\rho, \mathbf{\Delta}, u)$ is independent of u and $\mathbf{\Delta}$ for u sufficiently near a solution u^* of (4.1) and $\mathbf{\Delta}$ sufficiently small.

The main result of [5] is that if one wants to solve the equation for the Newton step for (4.4)

$$s - W^{\mathbf{\Delta}'}(u)s = -(u - W^{\mathbf{\Delta}}(u))$$

with GMRES, then the kth linear residual $r_{k,\mathbf{\Delta}}$ satisfies

$$\|r_{k,\mathbf{\Delta}}\|_{\mathbf{\Delta}} \leq C\rho^{k-N(\rho,\mathbf{\Delta},u)}\|r_{0,\mathbf{\Delta}}\|_{\mathbf{\Delta}}. \tag{4.6}$$

Hence, Theorem 4.1 will give a bound for the number of GMRES iterations needed to satisfy (4.3), and that bound will be independent of both $\mathbf{\Delta}$ and u if $\mathbf{\Delta}$ is sufficiently small and u is sufficiently near u^*.

The objective in the remainder of this section is to show how the discretizations used in [17–21, 28] can be expressed in the language of collective compactness.

4.2. Finite Dimensional Problems. In [16–20, 28] we approximated integrals in x with a Riemann sum or the trapezoid rule, integrals in k with the composite midpoint rule, solve (1.8) with a central difference, and discretize the spatial differential operator with the second-order BDF scheme [2]. The mesh spacing in x and k is uniform. We used Riemann sums rather than the trapezoid rule in [17–20, 28] to enable duplication of the results in [27], and used the trapezoid rule in x in [16]. Any discretization that uses only the nodal values in x and the midpoints of the intervals in k will satisfy Lemma 4.3.

To extend the discrete maps to the function spaces we will begin by defining approximating subspaces. We will divide $[-K, K]$ into an even number N_k intervals of length $\Delta_k = 2 * K/N_k$. We will denote the centers of the intervals by

$$k_l = -K + K * (2l-1)/N_k,\ l = 1, \ldots N_k.$$

We divide the interval $[0, L]$ into $N_x - 1$ intervals of length $\Delta_x = L/(N_x - 1)$. The endpoints of the intervals are

$$x_m = L(m-1)/(N_x - 1),\ m = 1, \ldots N_x.$$

We let

$$\mathbf{\Delta} = (\Delta_x, \Delta_k),$$

denote the mesh in x and k. Let

$$\bar{Z}^{\mathbf{\Delta}} : R^{N_x \times N_k} \to R^{N_x \times N_k}$$

be the discretization on Z for $V_{bias} > 0$ and

$$\bar{Z}_0^{\mathbf{\Delta}} : R^{N_x \times N_k} \to R^{N_x \times N_k}$$

be the discretization for $V_{bias} = 0$.

Let ϕ_m be the piecewise linear nodal basis function which is 1 at x_m and zero at x_p for $p \neq m$. We let χ_l be the characteristic function of the interval with center k_l. We define

$$X^{\mathbf{\Delta}} = \{f \in X \,|\, f(x,k) = \sum_{m,l=1}^{N_x,N_k} f_{ml}\phi_m(x)\chi_l(k)\},$$

so $f_{ml} = f(x_m, k_l)$. We define the map $\mathcal{P}^{\mathbf{\Delta}}$ from X to $X^{\mathbf{\Delta}}$ by

$$\mathcal{P}^{\mathbf{\Delta}} = \sum_{m,p,l=1}^{N_x,N_x,N_k} \chi_l(k)\phi_m(x)\pi_{mp} \int \chi_l(k')\phi_p(x')f(x',k')\,dx'\,dk'$$

where the coefficients π_{mp} are chosen so that $\mathcal{P}^{\mathbf{\Delta}}$ is the L^2 orthogonal projection in L^2 onto $X^{\mathbf{\Delta}}$. It is known that $\mathcal{P}^{\mathbf{\Delta}}$ converges strongly to the identity in each of L^2 and X. The map $\mathcal{P}^{\mathbf{\Delta}}$ can be used for both the zero-bias and nonzero-bias cases. We will also need an prolongation operator from $R^{N_x \times N_k}$ to $X^{\mathbf{\Delta}}$. To that end we define for $c \in R^{N_x \times N_k}$,

$$(\mathcal{Q}^{\mathbf{\Delta}}c)(x,k) = \sum_{m,l=1}^{N_x,N_k} c_{ml}\phi_m(x)\chi_l(k). \tag{4.7}$$

For the zero-bias case, we alter the prolongation to reflect the continuity and symmetry in k. For $k_1 \leq k \leq k_{N_k}$ we define

$$(\mathcal{Q}_0^{\mathbf{\Delta}}c)(x,k) = \sum_{m,l=1}^{N_x,N_k} c_{ml}\phi_m(x)\psi_l(k), + \sum_{m=1}^{N_x} \frac{c_{N_k/2,m} + c_{N_k/2+1,m}}{2}\phi_m(x)\psi_0(k),$$

where ψ_l is the piecewise linear basis function centered at k_l and ψ_0 the basis function centered at $k = 0$. This is a simple piecewise linear interpolation using the mesh points in x and k. Since the mesh points in k are the centers of the intervals, we must extend to all of $[-K, K]$, which we do by piecewise constants. So

$$(\mathcal{Q}_0^{\mathbf{\Delta}}c)(x,k) = (\mathcal{Q}_0^{\mathbf{\Delta}}c)(x,k_1)$$

if $k \leq k_1$ and

$$(\mathcal{Q}_0^{\mathbf{\Delta}}c)(x,k) = (\mathcal{Q}_0^{\mathbf{\Delta}}c)(x,k_{N_k})$$

if $k \geq k_{N_k}$. Finally we define the point evaluation map $\mathbf{E}^{\mathbf{\Delta}} : X^{\mathbf{\Delta}} \to R^{N_x \times N_k}$ by

$$\mathbf{E}^{\mathbf{\Delta}}(g)_{ml} = g(x_m, k_l). \tag{4.8}$$

We now describe how the differential operator D is discretized. For a given $\mathbf{\Delta}$ and mesh points $\{k_l\}$ and $\{x_m\}$, we use a second-order BDF to approximate the action of D on a function w at the node (x_m, k_l) by

$$(D^{\Delta_x})w(x_m,k_l) = -\frac{hk_l}{2m^*}\left(\frac{-3w(x_m)+4w(x_{m-1})-w(x_{m-2})}{2\Delta_x}\right), \tag{4.9}$$

and for $k_l < 0$ by

$$(D^{\Delta_x})w(x_m,k_l) = -\frac{hk_l}{2m^*}\left(\frac{3w(x_m)-4w(x_{m+1})+w(x_{m+2})}{2\Delta_x}\right). \tag{4.10}$$

In those cases where $x_{m\pm2}$ is outside the interval $[0, L]$, an implicit Euler discretization is used. We will require that the discretization be stable and consistent in x and k jointly. This point is a bit subtle. If we only seek to invert D, as we will in the computation of Z_0, then the division by k_l will cause no problems, as the symmetry of T will eliminate the singularity. In that case convergence of the map defined by (4.12) below will be in the uniform norm. However, in the nonzero bias case, we seek to invert $(I - \tau D^{\Delta_x})^{-1}$, and the convergence is not uniform in x and k together, but is rather in the discrete analog of the topology of X. We explore this in more detail in § 4.3.

We define the extended maps:

$$Z^{\mathbf{\Delta}}(f) = \mathcal{Q}^{\mathbf{\Delta}}\bar{Z}^{\mathbf{\Delta}}(\mathbf{E}^{\mathbf{\Delta}}(\mathcal{P}^{\mathbf{\Delta}}f)) \tag{4.11}$$

and

$$Z_0^{\mathbf{\Delta}}(f) = \mathcal{Q}_0^{\mathbf{\Delta}}\bar{Z}_0^{\mathbf{\Delta}}(\mathbf{E}^{\mathbf{\Delta}}(\mathcal{P}^{\mathbf{\Delta}}f)). \tag{4.12}$$

Because the discretization is consistent and convergent, and the interpolation and restriction maps use the same nodes as the discretization, the discrete problems, when mapped to the function space with the prolongations and projections defined above, converge strongly in the appropriate function space.

LEMMA 4.2. *The maps $Z^{\mathbf{\Delta}}$ and $Z_0^{\mathbf{\Delta}}$ converge strongly in X (resp X_0),* i. e. *For all $f \in X$,*

$$\lim_{\mathbf{\Delta}\to 0} Z^{\mathbf{\Delta}}(f) = Z(f),$$

in the norm of X. For all $f \in X_0$,

$$\lim_{\mathbf{\Delta}\to 0} Z_0^{\mathbf{\Delta}} = Z_0(f),$$

in the norm of X_0.

LEMMA 4.3. *$Z^{\mathbf{\Delta}}(f) = w$ for $w, f \in X^{\mathbf{\Delta}}$ if and only if $\bar{Z}^{\mathbf{\Delta}}(\mathbf{E}^{\mathbf{\Delta}}f) = \mathbf{E}^{\mathbf{\Delta}}w$. $Z_0^{\mathbf{\Delta}}(f) = w$ for $f \in X_0^{\mathbf{\Delta}}$ if and only if $\bar{Z}_0^{\mathbf{\Delta}}(\mathbf{E}^{\mathbf{\Delta}}f) = \mathbf{E}^{\mathbf{\Delta}}w$.*

Clearly $Z^{\mathbf{\Delta}}$ and $Z_0^{\mathbf{\Delta}}$ are uniformly (in $\mathbf{\Delta}$) Lipschitz continuously differentiable, because the nonlinearities are quadratic.

Lemmas 4.2 and 4.3 imply that the Newton iterations for the fully discrete problems will be equivalent to iterations for the associated problems on the finite dimensional function spaces in the sense that iterations for one can be mapped into iterations for the other with the maps $\mathbf{E}^{\mathbf{\Delta}}$, $\mathcal{Q}$, and $\mathcal{Q}_0$. Hence we can analyze the maps $Z^{\mathbf{\Delta}}$ and $Z_0^{\mathbf{\Delta}}$ using the tools of collective compactness and draw conclusions about algorithms which use the fully discretized maps $\bar{Z}_0^{\mathbf{\Delta}}$ and $\bar{Z}^{\mathbf{\Delta}}$.

Lemmas 4.2 and 4.3 are not enough to obtain the spectral properties we need to argue that the performance of the linear iteration is independent of the mesh parameter $\mathbf{\Delta}$. We must also show that the discretizations are collectively compact, *i. e.* the maps $Z^{\mathbf{\Delta}}$ (resp $Z_0^{\mathbf{\Delta}}$) map the unit ball in X (resp X_0) into a compact set in X (resp X_0) which is independent of $\mathbf{\Delta}$.

4.3. Collective Compactness. At this point we confine our discussion to the nonzero-bias case $f = Z(f)$. The zero-bias case is discretized in the same way, and the analysis differs only in that the symmetry, (1.11) and (3.10) in the zero-bias case make it possible to work in X_0 instead of X, as was the case in § 3.2.

THEOREM 4.4. *The family of maps $\{Z^{\mathbf{\Delta}}\}$ is collectively compact on X.*

Proof. Our proof of collective compactness follows the outlines of the compactness proof in § 3. We begin with the map that takes f to the discrete analog of Pf. If let $\bar{P}^{\mathbf{\Delta}}$ denote the discretization of P using the integration rules in x and k, and the central difference Poission solver. We extend $\bar{P}^{\mathbf{\Delta}}$ to a map on X with the evaluation and restriction maps defined in (4.7) and (4.8) to obtain

$$P^{\mathbf{\Delta}} = \mathcal{Q}^{\mathbf{\Delta}} P^{\mathbf{\Delta}} E^{\mathbf{\Delta}} \mathcal{P}^{\mathbf{\Delta}}. \tag{4.13}$$

The definition of P and properties of the discrete Greens function for the Laplacian [8] imply that the family of maps from $X \to C[-K, K]$,

$$\{f \to P^{\mathbf{\Delta}} f(x, \cdot) \,|\, \mathbf{\Delta}, x \in [0, L]\}$$

is collectively compact, *i. e.* compact in k, and bounded in x.

Similarly, if we let $Q^{\mathbf{\Delta}}$ be the interpolation to $X^{\mathbf{\Delta}}$ of the nodal values of the discrete form of Q via piecewise linear interpolation in x and piecewise constant interpolation in k, then the family $Q^{\mathbf{\Delta}}$ maps the unit ball in X to a bounded set in C which is equicontinuous in k.

So, to complete the proof, we need to show that the discrete inverses of $I - \tau D$ are a collectively compact family of maps from $C[0, L]$ to X. To make this precise let E^{Δ_x} be the evaluation map from $C[0, L] \to R^{N_x}$. Let D^{Δ_x} be defined by (4.9)–(4.10). Since the discretization is stable and consistent, the map $(I - \tau D^{\Delta_x})^{-1}$ is well-defined map from R^{N_x} to $R^{N_x \times N_k}$. We now need to show that the family

$$\{\mathcal{Q}^{\mathbf{\Delta}} (I - \tau D^{\Delta_x})^{-1} E^{\Delta_x} \,|\, \mathbf{\Delta} \text{ satisfies (4.15)}\} \tag{4.14}$$

is collectively compact. It suffices to assume that the boundary data are zero for this purpose, since convergence of the difference scheme implies that the discrete analogs of the terms corresponding to the boundary data in (3.11) converge.

We only will consider the case $k > 0$; the case for $k < 0$ is the same. We define $\bar{V}^{\mathbf{\Delta}} : R^{N_x}$ to $R^{N_x \times N_k}$ by

$$(\bar{V}^{\mathbf{\Delta}} c)_{lm} = \frac{\bar{c}}{k_l} ((I - \tau D^{\Delta_x})^{-1} c)_{ml},$$

We convert $\bar{V}^{\mathbf{\Delta}}$ to a map from $C[0, l]$ to X by

$$V^{\mathbf{\Delta}} = \mathcal{Q}^{\mathbf{\Delta}} \bar{V}^{\mathbf{\Delta}} E^{\Delta_x}.$$

We will complete our proof of collective compactness by showing that $V^{\mathbf{\Delta}}$ converges to V in the operator norm.

We will need to restrict

$$\Delta_x \bar{c} \le (3 - \bar{\epsilon}) \Delta_k, \tag{4.15}$$

for some $\bar{\epsilon} \ge 0$. If (4.15) holds, then it is a simple calculation to show that $V^{\mathbf{\Delta}}$ is a bounded operator from $C[0, L]$ into $L^\infty([0, L] \times [-K, K])$, *i. e.* there is C_1 such that

$$|V^{\mathbf{\Delta}} w(x, k)| \le C_1 \|w\|_\infty. \tag{4.16}$$

Convergence of the difference scheme implies that the operator $V^{\mathbf{\Delta}}$ is a degenerate kernel approximation of V, and that the convergence of the kernel functions of the operators is uniform for $x, y \in [0, L]$ and k bounded away from zero. So, for all $K_- \in (0, K]$,

$$\max_{x \in [0, L], k \in [K_-, K]} |(V^{\mathbf{\Delta}} - V) w(x, k)| = O(\|\mathbf{\Delta}\| \|w\|_\infty). \tag{4.17}$$

Similar ideas were used to develop multilevel methods in [12].

The two bounds (4.16) and (4.17) imply that

$$\|(V^{\mathbf{\Delta}} - V) w\|_X = O(\sqrt{K_-} + \|\mathbf{\Delta}\| \|w\|_\infty),$$

which, since we may choose K_- first and then reduce $\mathbf{\Delta}$, implies convergence of $V^{\mathbf{\Delta}}$ to V. This completes the proof. □

5. Conclusion. We have presented a rigorous analysis of the mathematical scalability of a preconditioner we have developed for the Wigner-Poisson equations and presented in previous papers [17–21, 28]. When showing the scalability of the preconditioner in the infinite-dimensional setting, we had to prove the preconditioned operator was compact, resorting in us using the obscure function space X. To show the preconditioner's scalability in the finite-dimensional case, we used the compactness of the preconditioned operator in the infinite-dimensional case and the fact that the finite-dimensional approximations strongly converged to their infinite-dimensional counterparts to show that the spectral properties in the infinite-dimensional case would be inherited by the finite-dimensional preconditioned operators. With this analysis, we are better able to understand the performance of the Newton-GMRES algorithm when applied to the preconditioned Wigner-Poisson equations and justify the use of these preconditioners in the zero bias and the nonzero-bias cases.

REFERENCES

[1] P. M. Anselone, *Collectively Compact Operator Approximation Theory*, Prentice-Hall, Englewood Cliffs, NJ, 1971.

[2] U. M. Ascher and L. R. Petzold, *Computer Methods for Ordinary Differential Equations and Differential Algebraic Equations*, SIAM, Philadelphia, 1998.

[3] B. A. Biegel, *Quantum Electronic Device Simulation*, PhD thesis, Stanford University, March 1997. Department of Electrical Engineering.

[4] F. A. Buot and K. L. Jensen, *Lattice Weyl-Wigner formulation of exact many-body quantum-transport theory and applications to novel solid-state quantum-based devices*, Phys. Rev. B, 42 (1990), pp. 9429–9457.

[5] S. L. Campbell, I. C. F. Ipsen, C. T. Kelley, and C. D. Meyer, *GMRES and the minimal polynomial*, BIT, 36 (1996), pp. 664–675.

[6] R. Dembo, S. Eisenstat, and T. Steihaug, *Inexact Newton methods*, SIAM J. Numer. Anal., 19 (1982), pp. 400–408.

[7] W. R. Frensley, *Wigner-function model of a resonant-tunneling semiconductor device*, Phys. Rev. B, 36 (1987), pp. 1570–1580.

[8] P. Henrici, *Discrete Variable Methods in Ordinary Differential Equations*, Wiley, New York, 1962.

[9] M. A. Heroux, R. A. Bartlett, V. E. Howle, R. J. Hoekstra, J. J. Hu, T. G. Kolda, R. B. Lehoucq, K. R. Long, R. P. Pawlowski, E. T. Phipps, A. G. Salinger, H. K. Thornquist, R. S. Tuminaro, J. M. Willenbring, A. Williams, and K. S. Stanley, *An overview of the trilinos project*, Tech. Rep. 3, Sandia National Laboratories, 2005.

[10] L. Kantorovich and G. Akilov, *Functional Analysis*, Pergamon Press, New York, second ed., 1982.

[11] H. B. Keller, *Lectures on Numerical Methods in Bifurcation Theory*, Tata Institute of Fundamental Research, Lectures on Mathematics and Physics, Springer-Verlag, New York, 1987.

[12] C. T. Kelley, *A fast multilevel algorithm for integral equations*, SIAM J. Numer. Anal., 32 (1995), pp. 501–513.

[13] ———, *Iterative Methods for Linear and Nonlinear Equations*, no. 16 in Frontiers in Applied Mathematics, SIAM, Philadelphia, 1995.

[14] ———, *Solving Nonlinear Equations with Newton's Method*, no. 1 in Fundamentals of Algorithms, SIAM, Philadelphia, 2003.

[15] C. T. Kelley and Z. Q. Xue, *GMRES and integral operators*, SIAM J. Sci. Comp., 17 (1996), pp. 217–226.

[16] M. S. Lasater, *Numerical Methods for the Wigner-Poisson Equations*, PhD thesis, North Carolina State University, Raleigh, North Carolina, 2005.

[17] M. S. Lasater, C. T. Kelley, A. Salinger, D. L. Woolard, and P. Zhao, *Enhancement of numerical computations of the Wigner-Poisson equations for application to the simulation of THz-frequency RTD oscillators*, in Proceedings of SPIE: Chemical and Biological Standoff Detection II Volume 5584, paper number 07, J. O. Jensen and J.-M. Theriault, eds., 2004, pp. 42–51.

[18] ———, *Parallel solution of the Wigner-Poisson equations for RTDs*, in 2004 International Symposium on Distributed Computing and Applications to Business, Engineering and Science, Q. Qingping, ed., Wuhan, China, 2004, Hubei Science and Technology Press, pp. 672–676.

[19] ———, *Parallel parameter study of the Wigner-Poisson equations for RTDs*, Computers and Mathematics with Applications, 51 (2006), pp. 1677–1688.

[20] M. S. Lasater, C. T. Kelley, A. Salinger, P. Zhao, and D. L. Woolard, *Simulating nanoscale devices*, International Journal of High Speed Electronics and Systems, 16 (2006), pp. 677–690.

[21] M. S. Lasater, C. T. Kelley, P. Zhao, and D. L. Woolard, *Numerical tools for the study of instabilities within the positive-differential-resistance regions of tunnelling devices*, in Proceedings of 2003 3nd IEEE Conference on Nanotechnology, San Francisco, CA, August 12–14, 2003, IEEE, 2003, pp. 390–393.

[22] Y. Saad and M. Schultz, *GMRES a generalized minimal residual algorithm for solving nonsymmetric linear systems*, SIAM J. Sci. Stat. Comp., 7 (1986), pp. 856–869.

[23] A. G. Salinger, N. M. Bou-Rabee, R. P. Pawlowski, E. D. Wilkes, E. A. Burroughs, R. B. Lehoucq, and L. A. Romero, *Loca 1.0 library of continuation algorithms: Theory and implementation manual*, Technical Report SAND2002-0396, Sandia National Laboratory, March 2002.

[24] I. Stakgold, *Green's Functions and Boundary Value Problems*, Wiley-Interscience, New York, 1979.

[25] E. Wigner, *On the quantum correction for thermodynamic equilibrium*, Phys. Rev., 40 (1932), pp. 749–759.

[26] Z. Q. Xue, *Mesh-independence of GMRES for Integral Equations*, PhD thesis, North Carolina State University, Raleigh, North Carolina, 1995.

[27] P. Zhao, H. L. Cui, and D. L. Woolard, *Dynamical instabilities and I-V characteristics in resonant tunneling through double barrier quantum well systems*, Phys. Rev. B, 63 (2001), p. 75302.

[28] P. Zhao, D. L. Woolard, M. S. Lasater, and C. T. Kelley, *Terahertz-frequency quantum oscillator operating in the positive differential resistance region*, in Proceedings of SPIE Defense and Security Symposium 2005: Terahertz for Military & Security Application III, paper number 5790-34, vol. 5790, 2005, pp. 289–300.